Supporting Information

SI Text

CPA transport across the cell membrane

In addition to the results of mass transport through cell membrane (Figures 2 (B)-(E)), the number of moles of CPAs during CPA loading/unloading steps were presented in Figures S1 (A) and (B). The standard one-step protocol offered the fastest increase and decrease in the number of CPA moles in the CPA loading and unloading steps, respectively. Such rapid change is most likely to cause osmotic shock to cells. In contrast, our microfluidic approach yields the slowest rate of change in CPA moles during CPA loading/unloading steps.

Cells traveling along the microfluidic channel

In our microfluidic approach, represented in Figure 1 (A), cells were injected into the middle of the microfluidic channel so that they are exposed to CPAs progressively. Figure S2 (A) illustrates the cells and CPAs infusing into the channel around the inlet of the microfluidic device, where we observed the interface between CPAs and PBS. When cells moved 0.8 m down the microfluidic channel, the flow interface disappeared (Figure S2 (B)). According to the particle migration theory, particles tend to move toward and to travel along the center of the channel because the center has the lowest energy state due to zero shear stress [1, 2]. Furthermore, the microfluidic system proposed in this study developed a stable laminar flow profile (Re ~ 3). These facts predict that cells will not stick to the microfluidic channel wall as they translate along a streamline, a result that is consistent with.experimental findings.

Supplementary tables

The parameters used in the numerical simulation are listed in Table S1 [3, 4]. We detailed the viability results as shown in Figure 4 (A) (Table S2). In the cryopreservation experiment, three independent samples were used for the two sample groups: standard cryopreservation protocol and our novel microfluidic method. The standard protocol involves 2 M one-step, 3 M one-step, and stepwise (1.5 M to 3 M) results. In the proposed microfluidic approach, 2 M and 3 M concentrations were studied. The values represent mean±SD. The standard deviation came from counting the images of live/dead tests. By comparing pre-freeze and post-thaw viabilities as shown in the table, we can observe the effects of osmotic shock during CPA loading and unloading steps.

1. B. H. Happel J, *Low Reynolds number hydrodynamics*, Noordhoff, Leyden, the Netherlands, 1973.
2. L. L. Ho BP, *Journal of Fluid Mechanics*, 1974, **65**, 365-400.
3. Z. F. Cui, R. C. Dykhuizen, R. M. Nerem and A. Sembanis, *Biotechnol Prog*, 2002, **18**, 354-361.
4. L. Y. Li, *Computational Materials Science*, 2006, **35**, 75-83.

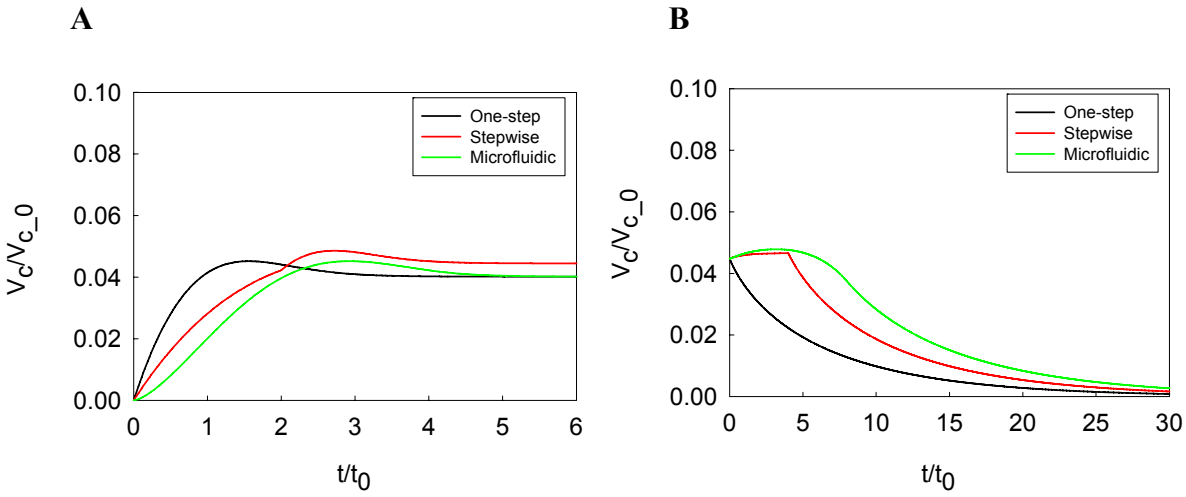

Figure S1. Change in the mole numbers of CPAs with respect to time. The dimensionless mole numbers of CPAs across cell membrane are presented during CPA loading (A) and CPA unloading steps. One-step, stepwise, and microfluidic loading/unloading cases were taken into account. The numbers were non-dimensionalized by using a characteristic mole number of CPA considered in this study, V_{c_0}.

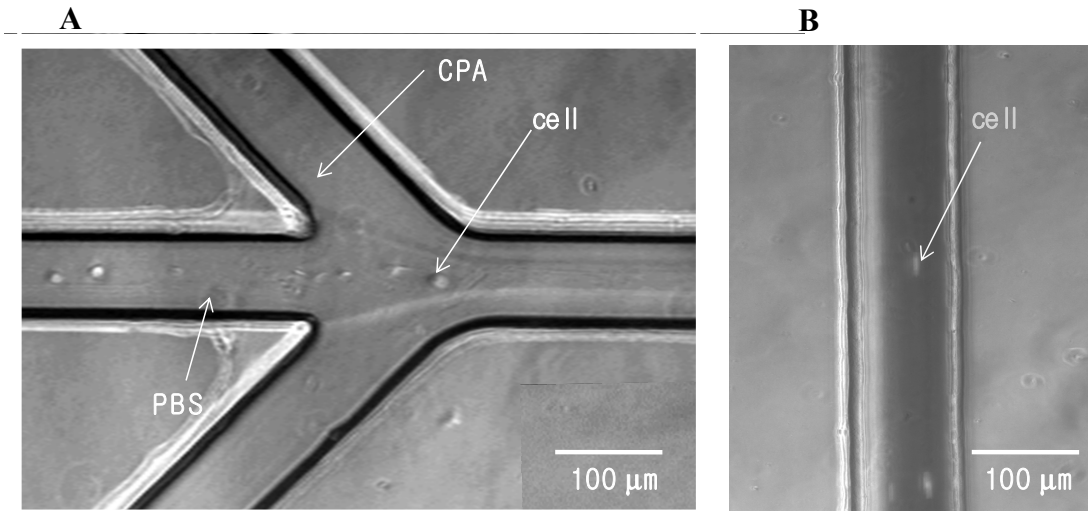

Figure S2. Bright field images of the microfluidic channel while CPA and PBS flow in the channel. (A) The cell-suspending PBS is infused through the middle of the microfluidic channel at the inlet, whereas the CPAs are injected through the two side channels. The cells move down along the PBS and then undergo CPAs progressively. (B) The image taken at a location, 0.8 m away from the inlet. The CPA solution diffuses toward the middle of the microfluidic channel as the cells travel through the channel.

Table S1. Model parameters used in computational simulation (3,4).

Parameters	**Values**	**Unit**
Membrane hydraulic conductivity (L_p)	6.09×10^{-15}	$m^3\ N^{-1}\ s^{-1}$
Membrane reflection coefficient (σ)	0.8	
Membrane permeability (ω)	1.08×10^{-15}	$kmol\ N^{-1}\ s^{-1}$
Universal gas constant and temperature (RT)	$8314\times(273+20)$	$Nm\ kmol^{-1}$
Elastic modulus (E)	1.0×10^{3}	$N\ m^{-2}$
Initial cell diameter (r_0)	1.0×10^{-5}	m
Initial pressure (P_0^i , P_0^e)	1.0×10^{5}	$N\ m^{-2}$
Final CPA concentration	3.0	M

Table S2. Viability of HepG2 cells measured in the experiments. Distinct cases of CPA concentration change during freezing and thawing were investigated. In each experiment, three different samples were prepared. This table presents detailed results of those shown in Figures 4 (A) and (B).

		Sample #1		**Sample #2**		**Sample #3**	
		Before freezing	After thawing	Before freezing	After thawing	Before freezing	After thawing
Standard cryopreservation	Initial flask	95.6±3.2[a]		91.9±2.1		93.5±2.2	
	2M one-step	89.9±1.0	58.8±2.1	85.7±1.1	52.6±2.1	88.2±3.6	55.2±1.9
	3M one-step	82.5±2.5	37.9±1.4	79.4±2.5	33.4±3.6	80.7±2.1	35.7±2.1
	1.5M to 3M stepwise	85.3±2.3	48.3±3.3	81.8±3.4	41.5±1.2	82.0±1.6	42.7±1.3
Proposed method	Initial flask	94.8±1.5		92.3±2.2		94.2±0.8	
	2M microfluidic	92.3±2.2	71.3±3.2	90.4±0.9	67.5±2.4	93.0±2.5	70.3±1.2
	3M microfluidic	90.5±1.8	65.4±2.7	89.3±3.0	60.4±3.2	91.9±1.8	64.2±2.0

[a] Mean ± SD